Fusion Engineering and Design 173 (2021) 112864

Contents lists available at ScienceDirect

Fusion Engineering and Design

journal homepage: www.elsevier.com/locate/fusengdes

Design of a 3.7 GHz, 1 kW CW hybrid radial power divider for LHCD system of SST-1 Tokamak

Sandeep R. Sainkar [a,1,*], Aviraj Jadhav [b], Alice N. Cheeran [a], J. John [b], Promod K. Sharma [c,2], Harish V. Dixit [d]

[a] Veermata Jijabai Technological Institute, Mumbai, Maharashtra 400019, India
[b] Indian Institute of Technology Bombay, Mumbai, Maharashtra 400076, India
[c] Institute for Plasma Research, Gandhinagar, Gujarat 382428, India
[d] BITS Pilani-Hyderabad Campus, Hyderabad, Telangana 500078, India

ARTICLE INFO

Keywords:
Resonant cavity
Suspended stripline
Radial power divider
High power
Phase imbalance

ABSTRACT

This paper presents a novel design of an 8-way radial power divider/combiner that exhibits low insertion loss and minimum phase imbalance. The proposed design is realized using combined features of resonant and non-resonant based power dividing/combining structures to reap the benefits of both kinds of designs. The multi-layered power divider is designed to operate at a frequency of 3.7 GHz for possible use in Lower Hybrid systems for fusion applications. The structure is simulated using COMSOL Multiphysics to evaluate its RF and thermal performance. Simulation results indicate that the proposed power divider exhibited an amplitude and phase imbalance of ±0.05 dB and ±0.1° respectively between the peripheral ports. The computed return loss for the input port of the power divider is around 56 dB while the insertion loss is approximately 0.24 dB. Coupled RF-thermal simulation results indicate the capability of this design to handle continuous wave (CW) power of up to 1 kW. The proposed device is intended to be narrowband and would be used in the 1 kW solid state RF source under development at the authors' institute.

1. Introduction

Vacuum tubes have been the preferred microwave source for high power applications in accelerators, tokamaks, and industrial ovens over the past few decades. Based on the type of the tube, they are capable to generate maximum power from a few kW to several hundreds of MWs in the pulsed or CW regime. However, due to the rapid developments in solid state technology, sources based on gallium nitride (GaN) devices are emerging to be an alternate source to replace the bulky tubes such as Klystrons, Traveling wave tubes, Gyrotrons, etc. [1,2]. Although solid state sources are efficient, reliable and economical, they have the limited capability of generating power, which is up to a few hundreds of watts at microwave frequencies. One way to obtain more power from these sources is to combine the power of several such sources in parallel, typically in a corporate-like structure [3,4]. Such scheme also gives an advantage of graceful degradation of power, wherein the system output power degrades gradually in case of failure of one or more sources. Using a combination of multiple solid state power sources thus seems to be advantageous as opposed to single or few very high power vacuum tubes. Hence, the authors undertook a study about the utility of high power solid state sources for fusion applications in current drive systems for tokamaks [5]. In [5], the authors have proposed a continuous wave (CW) solid state system operating at 3.7 GHz for applications in Lower Hybrid Current Drive (LHCD) of Steady State Superconducting Tokamak (SST-1). Such a system would require the use of power dividers as well as combiners in various stages. Power dividers would be required in the initial stages to ensure that the amplifiers in the succeeding stages do not operate in saturation, while power combiners would be needed in the final stage to combine the power of multiple amplifiers. This paper presents the design of a hybrid radial power divider/combiner (PDC), to be incorporated into the system proposed in [5]. A generic scheme of a combination of multiple moderate power sources for high power application is depicted in Fig. 1, showing the use of power dividers and combiners.

* Corresponding author.
E-mail address: sandeepsainkar@somaiya.edu (S.R. Sainkar).
[1] K J Somaiya College of Engineering, Vidyavihar, Mumbai, Maharashtra 400077, India
[2] Homi Bhabha National Institute, Mumbai, Maharashtra 400094, India

https://doi.org/10.1016/j.fusengdes.2021.112864
Received 7 January 2021; Received in revised form 31 August 2021; Accepted 2 September 2021
Available online 28 September 2021

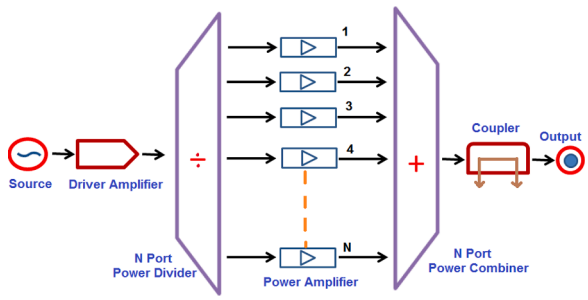

Fig. 1. Typical N-way divide and combine structure for high power microwave applications.

Table 1
Desired Specifications of Radial Power Divider.

Sr. No.	Parameters	Specifications
1.	Frequency of Operation	3.7 GHz (±5 MHz)
2.	Power handling capacity	Up to 1 kW
3.	Output VSWR at Rated Power @ 50 Ω	1.4: 1 max
4.	Input/output port impedance	50 Ω
5.	Insertion loss	< 0.5 dB
6.	Isolation	> 8 dB
7.	Power division	1: 8

Typically, PDC structures can be broadly classified into resonant (cavity) and non-resonant (non-cavity) structures preferred for narrowband and broadband applications, respectively. Various PDC techniques such as Corporate (series/multistep), *N*-way structures (parallel/single step) are reported in literature [3,4] [6–12]. Radial dividers/combiners are one of the predominant *N*-way type techniques, widely used due to their low loss and compact size. A suitable design of radial PDC depends upon the required bandwidth, size, isolation, and tolerances in amplitude and phase imbalance. In [7], the authors have presented an 8-way and 16-way radial non-resonant PDC, designed at 352 MHz, for up to 4 kW power. Herein the critical design of coaxial impedance matching sections increases the complexity of the structure. The authors of [8] have proposed a waveguide based radial PDC with a low insertion loss of 0.25 dB in the band of 27.5–31 GHz. It is compact in size, capable of handling high power but typically requires an accurate coaxial-waveguide transition. In [9], a non-resonant microstrip based 30-way radial PDC is described that exhibits an insertion loss of 0.55 dB and combining efficiency of around 90%. The lossy nature of the microstrip lines limits the combining efficiency in such structures. The 14:1 non-resonant power combiner design using a multi-layered dielectric structure reported in [10] comprises of a circular patch with 14 microstrip line peripheral ports, coupled through a Via to the bottom layer patch. It is suitable for wideband operation and has reduced structure complexity due to planar technology at the cost of dielectric losses. In contrast, an 8:1 resonant power combiner using a cylindrical cavity with suspended stripline is presented in [11]. The use of

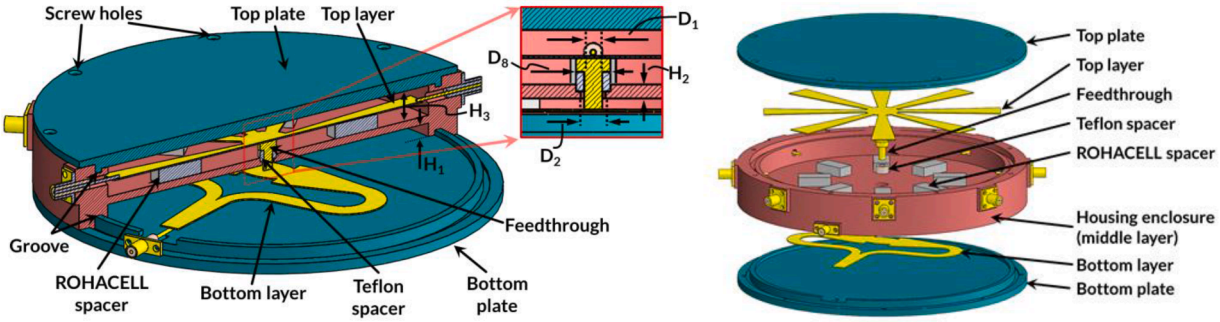

Fig. 2. 3-D labelled model of proposed 8-way power divider/combiner: (a) Cut section view (b) Exploded view.

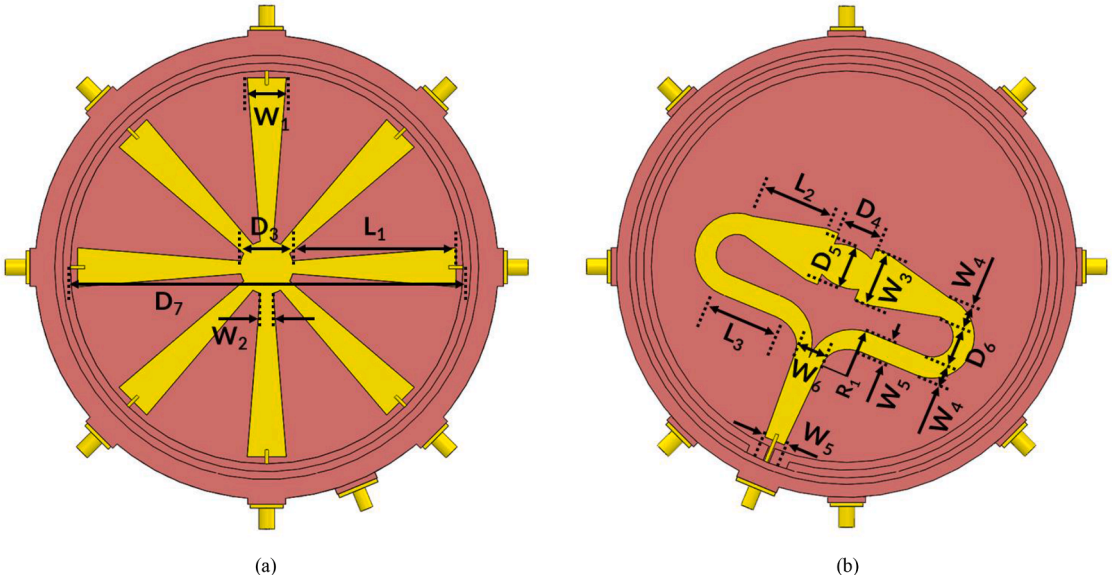

Fig. 3. Plan view of 8-way power divider/combiner showing (a) Top layer (b) Bottom layer.

Table 2
Design parameters of the proposed 8-way power divider.

Description	Parameter	Optimised value (mm)	Description	Parameter	Optimised value (mm)
Length of taper in top layer	L_1	72.75	Width of taper in bottom layer	W_3	21.4
Width of taper in top layer	W_1	15	Width of taper in bottom layer	W_4	8.2
Width of taper in top layer	W_2	5	Width of taper in bottom layer	W_5	8.1
Diameter of Coaxial feedthrough	D_1	4	Width of taper in bottom layer	W_6	11.4
Diameter of hole at middle layer	D_2	5.5	Height of bottom half of enclosure	H_1	5.5
Diameter of center disk	D_3	20.5	Thickness of middle layer (ground)	H_2	3.1
Length of taper in bottom layer	L_2	28.25	Height of upper half of enclosure	H_3	12.1
Length of taper in bottom layer	L_3	22.8	Thickness of taper stripline	T_1	0.5
Major diameter of elliptical disk	D_4	15.5	Diameter of cavity enclosure	D_7	151
Minor diameter of elliptical disk	D_5	16	Diameter of Teflon spacer	D_8	7.6
Diameter of Curved path	D_6	16.03			

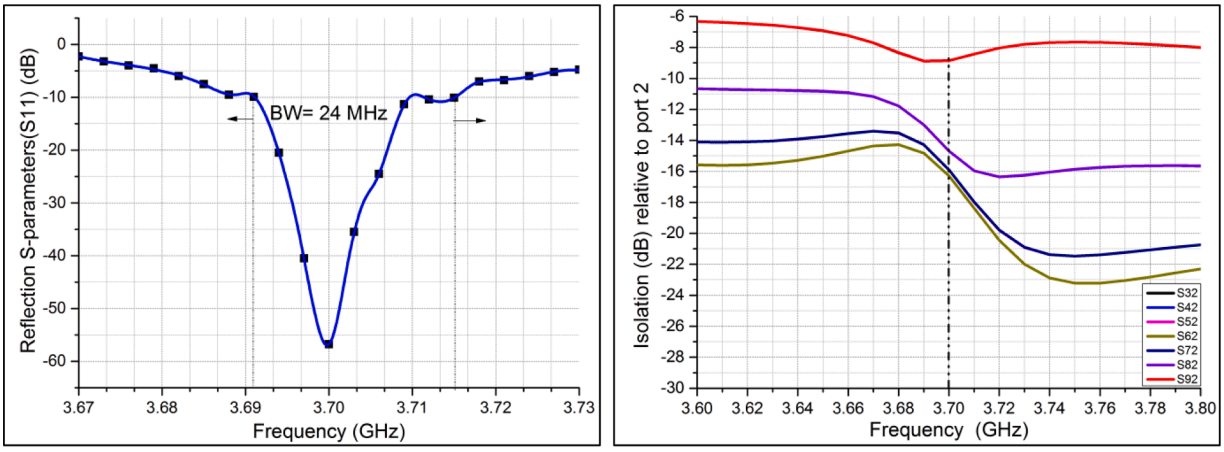

(a) (b)

Fig. 4. Simulated results (a) Reflection coefficient S-parameter (S11) (dB) at input port 1 as a function of the frequency (b) Isolation (Sn2) (dB) amongst the output peripheral ports (n = 3 to 9) with reference to port 2.

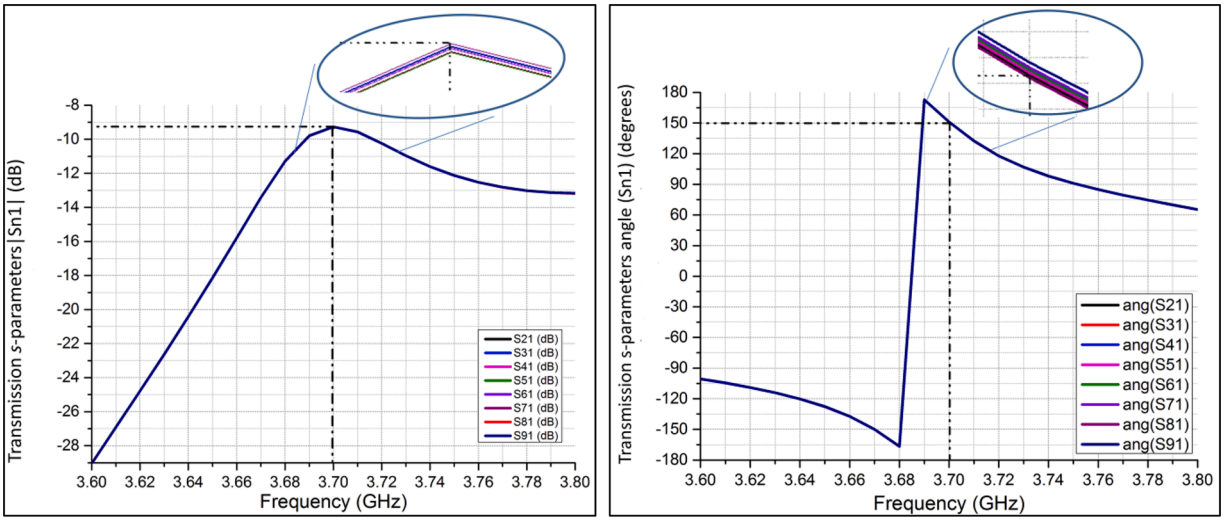

(a) (b)

Fig. 5. Simulated results of Transmission coefficient S-parameters (S_{n1}) (a) magnitude (dB) and (b) phase angle (degrees), when input port 1 is excited (n = 2 to 9).

suspended structure and cavity increases the power handling capacity and combining efficiency but needs precise machining work for practical implementation of the design. Another work [12] uses a suspended stripline made up of aluminium sheets supported in air substrate (loss-less dielectric) to achieve the power combination. The use of air as dielectric significantly reduces the dielectric losses. In summary, the non-resonant radial combiner uses a dielectric substrate (planar technology) and is preferred for wideband operation, improved isolation and its simple design at the expense of high losses in the combining medium. In contrast, the resonant radial combiners are preferred for its low loss and narrowband operation at the cost of relatively poor isolation, limited number of ports (up to 16), complexity in matching procedures.

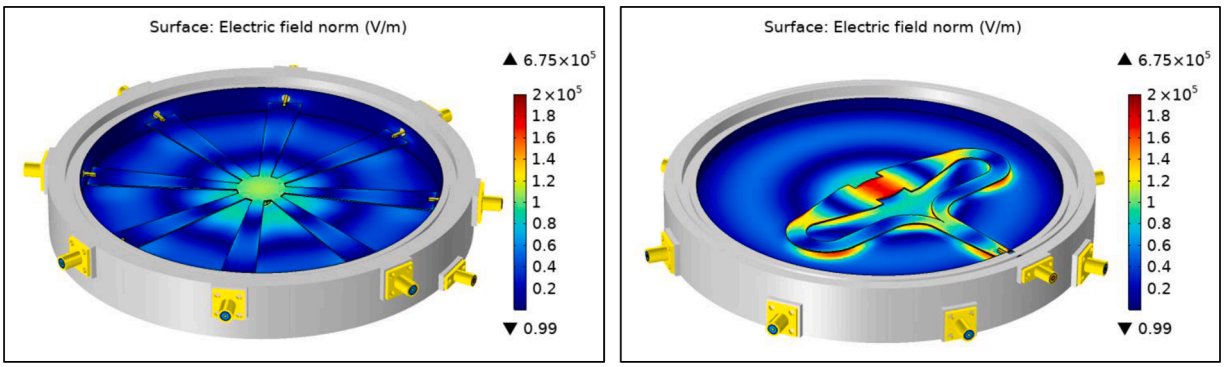

(a) (b)

Fig. 6. Electric field distribution for 8-way power divider (a) Top layer (b) Bottom layer, when input port 1 is excited with 1 kW CW power.
* The legend on the right side of the figure is scaled for better visualisation of the high and low field regions. The value at the top of the legend (6.75×10^5 V/m) indicate the maximum value of the E-field.

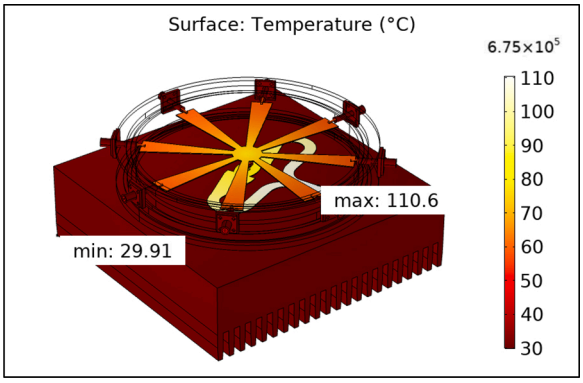

Fig. 7. Temperature distribution of 8-way power divider for 1 kW CW input power.

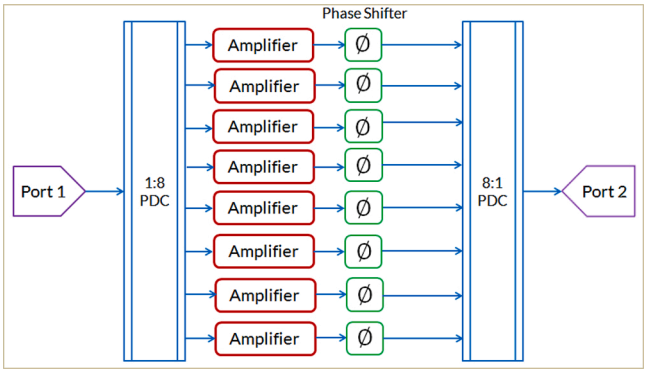

Fig. 8. Representation of simulated model to evaluate the effect of phase variations (imbalance) of the input signal on the gain of the PDC system.

Table 3
Effect of phase imbalance on the gain of PDC system

Phase Variation	Variation in gain	Statistical mean	Statistical deviation
±2°	±0.09 dB	18.035 dB	0.074
±5°	±0.22 dB	18.034 dB	0.039
±10°	±0.39 dB	18.022 dB	0.017

Additionally, they also exhibit an excellent power combining efficiency along with minimum phase and amplitude imbalance. The minimum imbalance amongst the inputs corresponds to low insertion loss, which in turn affects the combining efficiency [9]. Consequently, a radial PDC is advantageous for use in high power applications. A novel design of a CW hybrid radial power divider operating at 3.7 GHz is proposed in this work by combining the salient features of resonant and non-resonant [3,4,6] radial PDCs. The proposed structure is designated as 'hybrid' since it incorporates planar technology (simple construction) and cavity as a combining medium (high power handling, low loss). The desired specifications for the radial power divider are mentioned in Table 1.

The remainder of the paper is organised as follows. The design and structural details of the divider are described in section 2. In section 3, the simulation results are presented. The thermal simulation results are presented in section 4. Section 5 discusses about the results and the sensitivity analysis of the divider, while section 6 concludes the paper.

2. Structural details of power divider

The proposed power divider is a multi-layered structure comprising the top layer, middle layer, and bottom layer. The schematic view (cut section and exploded view) of the 8-way power divider is presented in Fig. 2. The top layer consists of eight taper striplines suspended in the air substrate. The taper lines are used to transform peripheral ports' low impedance to the high impedance at the center disk. This technique, as proposed in [10], is typically used to have a small radius of the power divider at the center. To further improve the power handling capacity and reduce the losses, a low loss suspended substrate stripline structure as proposed in [11,12] is preferred instead of microstrip line etched on the lossy dielectric substrate. The bottom layer comprises an elliptical shape stripline taper structure matched to the feed port impedance. The middle metal layer acts as a mutual ground between them, with a concentric hole at the center. The center disk at the top layer is directly coupled to the bottom layer stripline structure using a coaxial feedthrough conductor. A cylindrical Teflon spacer is placed in-between to isolate the coaxial feedthrough and middle ground plane, as shown in Fig. 2(b). The entire structure is confined into the housing enclosure, with the top and bottom plates covering the open sides. The cavity based design was preferable in our intended application as only narrowband operation is required. The selection of suitable material for the body of the cavity enclosure and taper striplines of the PDC depends on several factors [13]. In general, the electrical conductivity of metals is one of the dominant factors for an RF conducting body. Copper, brass, aluminium, gold, silver are considerably good choices, whereas steel alloys are preferred for high temperature applications. Amongst these materials, aluminium being more economical, relatively easy to fabricate, and highly conductive, is selected for this PDC.

Table 4
Comparison of state of art cavity and non-cavity based radial power dividers/combiners (Simulation results)

Ref.Paper	[10] (2019)	[15] (2015)	[16] (2014)	[13] (2017)	[11] (2011)	[17] (2014)	[18] (2013)	This Work
Combining medium	Microstrip	Cavity	Cavity	Partially filled Cavity	Suspended stripline + Cavity	Cavity	Microstrip	Suspended stripline + Cavity
No. of Combining ports	14	6	8	16	8	8	19	8
Type of port interface (input/output)	Microstrip/ Microstrip	Microstrip/ Waveguide	Waveguide/ Coaxial	Microstrip/ Coaxial	Microstrip/ Coaxial	Waveguide/ Coaxial	Microstrip/ Coaxial	Microstrip/ Microstrip
Operating frequency f_0 (GHz)	1.1 - 6	9.65	8 - 12	4	12.1 - 15.7	7.5 - 10.5	1.98 - 2.67	3.7
Insertion loss (dB)	< 2	< 0.3	< 0.3	< 0.3	0.17	< 0.2	0.9	0.24
Return loss (dB)	≥ 10	20	≥ 16	18	≥ 15	≥ 15	≥ 17	56.2
Isolation (dB)	≥ 8.6	-	-	-	≥ 7	≥ 11	≥ 10.5	≥ 9
Amplitude imbalance (dB)	± 0.75	-	-	± 0.2	± 0.5	± 0.1	-	± 0.05
Phase imbalance (degrees)	± 4.5	-	-	± 2	-	± 0.5	-	± 0.1
Power handling capacity	Up to 100 W (CW)	-	> 600 W (Peak power)	> 100 W (CW)	-	-	-	Up to 1 kW (CW)

The mechanical aspect of the design is also crucial and appropriate considerations are required to be incorporated before the fabrication of the design. Enough care must be taken to avoid any short or unnecessary gaps while integrating several parts of the PDC. The top and bottom plates (lid cover) of the enclosure can be tightened with screws at appropriate locations, as shown in Fig. 2(a), such that they do not affect the electrical characteristics of the design. Grooves are incorporated on the enclosure walls such that they fit and align perfectly with the ring-shaped protrusions on the top and bottom plates and also avoid any leakage of fields. The suspended stripline layers inside the enclosure can be supported with ROHACELL spacer whose dielectric constant is very close to air and has a minimum loss tangent. The fabrications of stripline, metallic cavity and their positioning must be within the acceptable tolerance limit (10–20 μm) to avoid undesirable imbalance. The layer-wise detailed description of the internal structure is given in the following subsections.

2.1. Top Layer

The top layer comprises of eight taper lines connected to the center of the divider. All these lines are also attached to 8 peripheral coaxial output ports at the other end. Each peripheral port impedance was transformed from 50 Ω to 100 Ω through these taper lines so that the net impedance at the center is (100Ω/8) 12.5 Ω. The tapered stripline design at the top layer is suspended in the air substrate between the two ground planes with a gap height (H_3). Here the top cover-lid of the enclosure and the middle layer conducting disk together acts as ground planes. The initial width of the stripline (W_1, W_2) is calculated for the given characteristic impedance Z_0. Also, these lines meet at the center disk of diameter (D_3) on the output side of the divider, as depicted in Fig. 3(a). The diameter of the disk is an important element for achieving significant return loss at the desired operating frequency of 3.7 GHz. Hence it is optimised along with the length of taper lines (L_1) to achieve the desired results. The initial value (D_7) is decided using Eq. (1) to ensure that the cavity resonates with TM_{01} mode while TM_{02} mode is in cut-off at the desired operating frequency. Here $f_{max} = 3.75$ GHz, $f_{min} = 3.65$ GHz, $n = 0$ and $m = 1$, p_{nm} is the m^{th} root of $J_n(x)$ (Bessel function of first kind), ε and μ are the permittivity and permeability of the dielectric, respectively.

$$\frac{p_{nm}}{2\pi f_{min}\sqrt{\mu\varepsilon}} < D_7 < \frac{p_{nm}}{2\pi f_{max}\sqrt{\mu\varepsilon}} \quad (1)$$

2.2. Middle layer

A coaxial feedthrough cylindrical conductor passes through a hole in the middle layer conducting disk of diameter (D_7) (acting as a common ground plane for top and bottom layer designs). The spacing between the coaxial feedthrough and the disk must be tuned for proper impedance matching at the center of the top and bottom layer stripline. The diameter (D_1) of coaxial feedthrough is optimised such that its characteristic impedance matches the impedance of the center disk. This provides the smooth transition from the top layer radial stripline to the bottom layer stripline.

2.3. Bottom layer

This layer forms the input section of the power divider consisting of a 50 Ω coaxial port used as a launcher port. The coaxial feedthrough meets the bottom layer at the center, whose impedance is 12.5 Ω. A single direct taper line to match both these impedances would be difficult to realise [10] due to the size constraint posed by the enclosure size which is fixed on account of the taper length transitions from 50 Ω to 100 Ω in the top layer. So the center portion is further extended through two split lines, as shown in Fig. 3(b). These lines would then have the characteristic impedance of 25 Ω, which are then combined and gradually transformed to a 50 Ω feeder line. The tapered stripline lengths (L_2, L_3) are further optimised such that they fit within the enclosure.

3. Simulated results

The RF and thermal performance of the power divider are evaluated using COMSOL Multiphysics software. The software was selected for its ability to couple multiple physics like electromagnetics (EM), thermal and fluid flow. In order to compute the *S*-parameters and E-fields, the '*EM Waves, Frequency Domain (emw)*' physics interface was used in COMSOL. All the internal metal surfaces of the design were assigned the '*impedance boundary condition*'. This boundary condition helps simulate the effect of skin depth on the metal surfaces without the need for meshing inside metals. Coaxial lumped ports with an impedance of 50 Ω were assigned to the input and output ports. An appropriate 3-D model of connectors can be selected by considering the physical dimensions of the available connectors mentioned in the datasheet and their power handling capacity. During the simulation, the impedance at the coaxial feedthrough is determined initially. This value is then used to tune the tapered striplines for impedance matching. After carrying out successive iterations and optimisations, the dimensions of different parts of the

geometry were finalized to obtain appropriate *S*-parameters suited for the power divider. Table 2 shows the optimised values of all the dimensions after fine-tuning. With the excitation at the input port of the divider, the simulated return loss is observed to be approximately 56.76 dB at 3.7 GHz, as shown in Fig. 4(a). It also shows a 10 dB bandwidth of 24 MHz over a frequency range (3.69–3.71 GHz). The isolation for the diametrically opposite ports of the combiner is observed to be above 9 dB over the desired bandwidth, whereas it is above 15 dB for the remaining adjacent ports, as depicted in Fig. 4(b). As the design is planned for operation at high power, the use of isolation resistors is avoided. However, isolation can be further improved by using some reactive elements [14] at the cost of insertion loss.

Due to the air-filled cylindrical cavity, the PDC exhibits almost zero dielectric losses as compared to [10]. The ideal value of transmission (coefficient) *S*-parameters (S_{n1}) for an 8-way power divider is around -9.03 dB. Fig. 5(a) shows the average value of transmission *S*-parameters to be approximately equal to -9.27 dB, which corresponds to an insertion loss of around 0.24 dB at the desired operating frequency of 3.7 GHz. Another model of PDC was built with the output ports of the divider connected to input ports of the combiner, which resembles a back-to-back PDC structure. The model was then simulated to verify the insertion loss and to determine the losses due to phase imbalance. The combined insertion loss was found to be 0.5 dB at a frequency of 3.7 GHz. Since individual 8-way PDC exhibit insertion loss of 0.24 dB, the loss due to phase imbalance is 0.02 dB, which is relatively low. The combining efficiency was then found to be more than 95%. It also exhibits a minimum amplitude imbalance of ±0.05 dB among the peripheral ports, as estimated from Fig. 5(a). The average phase imbalance is found to be within ±0.1° as computed (with reference to the phase angle at port 5) from Fig. 5(b); hence, the proposed design of the power divider is suitable 8-way configuration for high power low-loss applications.

4. Thermal analysis

The EM-thermal co-simulation is performed to account for the thermal behaviour of the designed power divider. The power handling capability of the proposed design can be determined by examining the electric field distribution within the structure, as shown in Fig. 6. For the applied input power of 1 kW CW, the maximum electric field of 0.675 MV/m is found to be concentrated around the edges of the input feed line as well as at the center of the bottom layer. It is far below the typical electric breakdown threshold voltage of air dielectric (3 MV/m). This ensures that the proposed device is capable of withstanding more than 1 kW CW with the point of view of RF breakdown. To observe the heating effect due to the high power input, all the domains were added in the '*Heat Transfer in Solids (ht)*' physics interface of COMSOL. Convective heat flux was assigned to the external boundaries with a heat transfer coefficient of 5 W/(m^2K). This imitates the practical condition of convective heat transfer between the metal surfaces and surrounding air. The solution from the '*emw*' physics was linked to '*ht*' using the *Multiphysics* node in COMSOL. After using the '*Frequency-stationary*' solver to obtain the solution at steady state condition, the maximum temperature without heatsink was observed to be around 170 °C. The divider was then modelled to be mounted on a finned heat sink of size (191.9 × 55.9 mm), having a total of 22 fins. The heat sink is initially assumed to be naturally cooled by applying constant heat flux boundaries. Assuming an ambient temperature of 25 °C, a thermal simulation was performed. Fig. 7 shows the temperature distribution profile for an input of 1 kW CW power. The maximum temperature (with heatsink and natural cooling) around the feeder port is found to be 110 °C. Further improvement in the thermal performance may be achieved by forced air cooling.

5. Discussion

A lossless and perfectly matched power combiner would yield maximum output power with the highest combining efficiency. However, slight deviations in fabrication, impedance mismatch, and phase offset of the input signals may lead to some imbalance in amplitude and phase. This imbalance reduces the overall combining efficiency. Hence, there is always a need to determine the performance sensitivity of the designed device before fabrication. Fig. 8 represents the simulated model to evaluate the effect of phase variations of the input signal on the output power and gain of the PDC system. *S*-parameters of the designed PDC were imported in Cadence Microwave Office (MWO) software [19]. Linear gain amplifier design, as reported in [5], was connected to each peripheral output port of the divider. The cascaded gain under ideal conditions is assumed to be approximately 18 dB. Phase shifters had been incorporated along the path to model the effect of phase variation. The phase of each shifter was varied over a Gaussian distribution for a phase tolerance limit of ±2°, ±5°, and ±10°. Monte Carlo (yield) simulations were performed to evaluate the combiner sensitivity for 200 iterations. Table 3 shows the average mean and variation (standard deviation) of output gain with a change in phase of the input signals. It has been observed that the deviation in gain is approximately ±0.4 dB for a phase change of ±10°, which may not be recommended as per the desired specifications. In comparison, phase variations of ±5° allow less deviation in gain up to ±0.2 dB, which is acceptable for low loss applications.

Table 4 shows the comparison of this work with some of the simulation results of cavity based and non-cavity based radial PDC from the literature. It can be observed that the proposed work shows good performance as compared to other sources available in the literature. It has all the combined features of the cavity and non-cavity based radial power dividers. This design would be well-suited for narrowband high power applications. It exhibits very low amplitude and phase imbalance along with low insertion loss. Isolation amongst the peripheral ports is also comparable to that of the existing designs.

6. Conclusion

The hybrid design of an 8-way power divider at 3.7 GHz is discussed. The resonant cavity structure and use of air as dielectric enhances the power handling capacity of the divider and minimizes the insertion loss. The use of planar technology for power combining reduces the need for precision machining work. Bandwidth of the divider is observed to be around 24 MHz, with an isolation of more than 9 dB among the peripheral ports. The design exhibits a low insertion loss of 0.24 dB and high combining efficiency of more than 95%. The phase imbalance was found to be within ±0.1°, which is comparable to the existing designs in the literature. The thermal analysis provided satisfactory results, thereby confirming the capability of the divider to withstand high power input. Mechanical constraints and fabrication tolerances are evaluated by carrying out a sensitivity analysis. Fabrication of the proposed design is in progress and details of the measured results would be reported later.

CRediT authorship contribution statement

Sandeep R. Sainkar: Formal analysis, Software, Investigation, Writing – original draft. **Aviraj Jadhav:** Software, Investigation. **Alice N. Cheeran:** Methodology, Resources, Supervision, Funding acquisition, Project administration. **J. John:** Resources, Supervision. **Promod K. Sharma:** Methodology, Supervision, Funding acquisition, Project administration. **Harish V. Dixit:** Conceptualization, Supervision.

Declaration of Competing Interest

The authors declare that they have no known competing financial

interests or personal relationships that could have appeared to influence the work reported in this paper.

Acknowledgments

The authors would like to acknowledge the Board of Research in Nuclear Sciences-Plasma and Fusion Research Committee (BRNS-PFRC) and National Fusion Programme (NFP) for supporting the project with a grant [39/14/09/2018]. The simulations for the work discussed in the paper were performed on ANTYA, an IPR Linux cluster. The authors would like to convey thanks to the IPR (Gandhinagar) team for the use of cluster and COMSOL Multiphysics software. Also, special thanks to VJTI Mumbai, K J Somaiya College of Engg. Mumbai and BITS-Pilani Hyderabad Campus for providing required resources.

References

[1] G. Formicone, J. Burger, J. Custer, G. Bosi, A. Raffo, G. Vannini, Solid-state RF power amplifiers for ISM CW applications based on 100 V GaN technology, in: Proceedings of the 11th European Microwave Integrated Circuits Conference (EuMA), 2016.
[2] P. Marchand, Review and prospects of RF solid state power amplifiers for particle accelerators, Proc. IPAC (2017).
[3] K.J. Russel, Microwave power combining techniques, IEEE Trans. Microwave Theory Tech. 27 (5) (1979) 472–478.
[4] K. Chang, C. Sun, Millimeter-wave power-combining techniques, IEEE Trans. Microwave Theory Tech. 31 (2) (1983) 91–107.
[5] S.R Sainkar, A.N. Cheeran, M. Reddy, H.V. Dixit, P.K. Sharma, Design of the 3.7 GHz, 1 kW CW solid state driver for LHCD system of the SST-1 Tokamak", Fusion Engineering and Design, 158, Elsevier, 2020.
[6] J. Schellenberg, The evolution of power combining techniques: from the 60s to today, IEEE MTT-S Int. Microwave Sympos. (2015).
[7] A. Jain, D.K. Sharma, A.K. Gupta, P.R. Hannurkar, High Power Low Loss Radial RF Power Dividers/Combiners, APAC (2007) 520–522.
[8] G. Zhai, B. Shi, Compact low loss millimetre wave 8-way radial waveguide power combiner, in: Proceedings of the 2017 IEEE Region 10 Conference (TENCON), 2017.
[9] A.E. Fathy, S. Lee, D. Kalokitis, A simplified design approach for radial power combiners, IEEE Trans. Microwave Theory Tech. 54 (1) (2006).
[10] S. Hossein, J. Hosseini, V. Nayyeri, Printed circuit board implementation of wideband radial power combiner, IEEE Access 7 (2019) 83536–83542.
[11] X. Shan, Z. Shen, A suspended-substrate Ku-band symmetric radial power combiner, IEEE Microwave Wireless Compon. Lett. 21 (12) (2011) 652–654.
[12] A.F. Elshafey, M.A. Abdalla, Low loss high power air suspended stripline power divider for high power division sub-systems applications, Prog. Electromagnet. Res. 73 (2018) 153–162.
[13] M. Ghanadi, H. Henke, A. Banai, A compact broadband N-way microstrip radial power combiner, in: 7th German Microwave Conference (GeMic), 2012.
[14] H.J. Du Toit, D.I.L. De Villiers, A fully isolated N-way radial power combiner, IEEE Trans. Microwave Theory Tech. 68 (7) (2020).
[15] V. Ravindra, H. Saito, J. Hirokawa, M. Zhang, Cylindrical cavity microwave power combiner with microstrip line inputs and rectangular, waveguide output, IEEE MTT-S Int. Microwave Sympos. (2015).
[16] X. Li, G. Chen, M. Zhan, R. Xu, A new planar compatible power combiner based on radial waveguide, IEEE Int. Conf. Commun. Problem-Solving (2014).
[17] A.A. Sarhan, N. Ghadimi, E. Hamidi, H. Oraizi, Broadband radial waveguide power combiner with improved isolation among adjacent output ports, Prog. Electromagnet. Res. 51 (2014) 63–70.
[18] W.Wang Fan, Z. Yan, A novel 1:19 microstrip radial power divider design for the application in antenna array, IEEE Int. Workshop Microwave Millimeter Wave Circuits Syst. Technol. (2013).
[19] Cadence AWR, Design environment user's guide, Microwave office, 2021.